

Perpendicular magnetic anisotropy of Pd/Co_2MnSi/Co/Pd multilayer

Xiaoqi Qin(秦晓奇), Jiaxing Tan(谭家兴), Xianwu Xiu(修显武), Wentian Cao(曹文田), and Shuyun Wang(王书运)

Citation: Chin. Phys. B, 2025, 34 (**3**): 037502. DOI: 10.1088/1674-1056/ada694
Journal homepage: http://cpb.iphy.ac.cn; http://iopscience.iop.org/cpb

What follows is a list of articles you may be interested in

Room-temperature creation and manipulation of skyrmions in MgO/FeNiB/Mo multilayers

Wen-Hui Liang(梁文会), Jian Su(苏鉴), Yu-Tong Wang(王雨桐), Ying Zhang(张颖), Feng-Xia Hu(胡凤霞), and Jian-Wang Cai(蔡建旺)

Chin. Phys. B, 2023, 32 (**12**): 127504. DOI: 10.1088/1674-1056/acf5d4

Electric-field control of perpendicular magnetic anisotropy by resistive switching via electrochemical metallization

Yuan Yuan(袁源), Lu-Jun Wei(魏陆军), Yu Lu(卢羽), Ruo-Bai Liu(刘若柏), Tian-Yu Liu(刘天宇), Jia-Rui Chen(陈家瑞), Biao You(游彪), Wei Zhang(张维), Di Wu(吴镝), and Jun Du(杜军)

Chin. Phys. B, 2023, 32 (**6**): 067505. DOI: 10.1088/1674-1056/acbde8

Charge-mediated voltage modulation of magnetism in $Hf_{0.5}Zr_{0.5}O_2$/Co multiferroic heterojunction

Jia Chen(陈佳), Peiyue Yu(于沛玥), Lei Zhao(赵磊), Yanru Li(李彦如), Meiyin Yang(杨美音), Jing Xu(许静), Jianfeng Gao(高建峰), Weibing Liu(刘卫兵), Junfeng Li(李俊峰), Wenwu Wang(王文武), Jin Kang(康劲), Weihai Bu(卜伟海), Kai Zheng(郑凯), Bingjun Yang(杨秉君), Lei Yue(岳磊), Chao Zuo(左超), Yan Cui(崔岩), and Jun Luo(罗军)

Chin. Phys. B, 2023, 32 (**2**): 027504. DOI: 10.1088/1674-1056/ac9a3b

Thickness-dependent magnetic properties in Pt/$[Co/Ni]_n$ multilayers with perpendicular magnetic anisotropy

Chunjie Yan(晏春杰), Lina Chen(陈丽娜), Kaiyuan Zhou(周恺元), Liupeng Yang(杨留鹏), Qingwei Fu(付清为), Wenqiang Wang(王文强), Wen-Cheng Yue(岳文诚), Like Liang(梁力克), Zui Tao(陶醉), Jun Du(杜军),Yong-Lei Wang(王永磊), and Ronghua Liu(刘荣华)

Chin. Phys. B, 2023, 32 (**1**): 017503. DOI: 10.1088/1674-1056/ac5c37

Perpendicular magnetization and exchange bias in epitaxial NiO/$[Ni/Pt]_2$ multilayers

Lin-Ao Huang(黄林傲), Mei-Yu Wang(王梅雨), Peng Wang(王鹏), Yuan Yuan(袁源), Ruo-Bai Liu(刘若柏), Tian-Yu Liu(刘天宇), Yu Lu(卢羽), Jia-Rui Chen(陈家瑞), Lu-Jun Wei(魏陆军), Wei Zhang(张维), Biao You(游彪), Qing-Yu Xu(徐庆宇), and Jun Du(杜军)

Chin. Phys. B, 2022, 31 (**2**): 027506. DOI: 10.1088/1674-1056/ac2b22

Perpendicular magnetic anisotropy of $Pd/Co_2MnSi/Co/Pd$ multilayer

Xiaoqi Qin(秦晓奇), Jiaxing Tan(谭家兴), Xianwu Xiu(修显武),
Wentian Cao(曹文田)[†], and Shuyun Wang(王书运)[‡]

School of Physics and Electronics, Shandong Normal University, Ji'nan 250358, *China*

(Received 5 September 2024; revised manuscript received 17 December 2024; accepted manuscript online 7 January 2025)

Pd/Co_2MnSi (CMS)/Co/Pd multilayer films were designed based on the idea of combining highly spin-polarized materials with strong perpendicular magnetic anisotropy (PMA) films. The PMA of Pd/CMS/Co/Pd multilayer films was studied by optimizing the growth conditions and thickness of each film layer. The optimal structure of the multilayer films was Pd(6 nm)/CMS(5 nm)/Co(2 nm)/Pd(1 nm). Its abnormal Hall resistance ($R_{\rm Hall}$), coercivity ($H_{\rm c}$) and effective magnetic anisotropy constant ($K_{\rm eff}$) are 0.08 Ω, 284 Oe and 1.36 Merg/cm^3, respectively, which are 100%, 492%, and 183% higher than the corresponding values (0.04 Ω, 48 Oe, and 0.48 Merg/cm^3) of the Pd(6 nm)/Co(1 nm)/Pd(3 nm) trilayer films. The analysis shows that the increases of the above values are the result of the Pd/CMS interface effect and CMS/Co interface ferromagnetic (FM) coupling, and that it is closely related to the thickness of each film layer in the multilayer films and the growth conditions of the multilayer films.

Keywords: perpendicular magnetic anisotropy (PMA), Co_2MnSi (CMS), Co, abnormal Hall resistance ($R_{\rm Hall}$), coercivity ($H_{\rm c}$)

PACS: 75.30.Gw, 75.50.Gg, 75.70.–i, 75.75.–c

DOI: 10.1088/1674-1056/ada694 **CSTR:** 32038.14.CPB.ada694

1. Introduction

With the rapid development of magnetic storage technology, the requirements for memory capacity and storage speed have increased. Spin transfer torque-magnetic random access memory (STT-MRAM) based on perpendicular magnetic anisotropy (PMA) materials has great application potential in high density magnetic recording media. This has aroused great interest in research on PMA materials.[1–4] For STT-MRAM, one of the current important research tasks is to improve the magnetic storage density.[5,6] Therefore, large PMA is required for the film.

Up to the present date, some relevant studies on PMA materials have focused on rare earth transition metal films,[7–10] L10 ordered alloy films[11–14] and ferromagnetic (FM)/nonmagnetic multilayer films.[15–18] However, these thin film structures all suffer from the problem of low spin polarizability. Co_2MnSi (CMS) has 100% spin polarization, a low damping coefficient, high Curie temperature, and high thermal stability.[19–23] However, PMA does not exhibit in the single CMS alloy film. Relevant experiments report that PMA emerges in FM/FM multilayer film structures due to the exchange coupling effect between layers.[24–26] Co itself has spin–orbit coupling and perpendicular magnetic anisotropy.[27] The implementation of PMA in CMS/Co multilayer film structures has not been reported. In 2018, Haifeng *et al.* reported that the interfacial spin flow transmission loss is almost 0 when strong spin–orbit coupled material Pd is combined with FM materials Co and CoFe, etc. Interface regulation can effectively improve the efficiency of spintronics devices.[6,28]

Therefore, in this paper, CMS alloy with high spin polarizability and Co thin film material with PMA are combined. Pd is selected as the heavy metal (HM) bottom layer and top protective layer, and the Pd/CMS/Co/Pd multilayer films are systematically studied.

2. Experiment

In this experiment, Pd/CMS/Co/Pd multilayer films were prepared. All samples were deposited on Corning glass substrate by magnetron sputtering. The background vacuum of the sputtering system is better than 1×10^{-3} Pa before sputtering the multilayer films. The substrate rotates at 15 rpm during the sputtering process to ensure that the sputtered particles can be uniformly sputtered onto the Corning glass substrate. Experimental variables for preparing multilayer films are shown in Table 1 and sputtering parameters for each target are shown in Table 2 (symbols or numbers in parentheses represent the thickness of each layer of film, measured in nanometers). In this experiment, the sputtering rates of Pd, CMS and Co targets are measured by the mass weighing method.[29] Their sputtering rates are 0.18 nm/s, 0.22 nm/s and 0.022 nm/s, respectively. The Hall effect of the multilayer films is measured by

[†]Corresponding author. E-mail: caowentian@sdnu.edu.cn
[‡]Corresponding author. E-mail: wangshuyun65@163.com

© 2025 Chinese Physical Society and IOP Publishing Ltd. All rights, including for text and data mining, AI training, and similar technologies, are reserved.

the four-probe method and the applied magnetic field is perpendicular to the film surface. The sample used to measure the Hall effect is shaped as a Hall rod, and the measurement is performed at room temperature with an injection current of 5mA. The hysteresis loops of multilayer films are measured with an alternating gradient magnetometer (MicroMag 2900).

Table 1. Series of multilayer films and corresponding experimental variables.

Experimental structure	Experimental variables
Pd(6)/Co(t_{Co})/Pd(3)	Co layer thickness: $t_{Co} = 0.5$, 1, 2, 3 nm
Pd(6)/CMS(t_{CMS})/Co(2)/Pd(3)	CMS layer thickness: $t_{CMS} = 1$, 2, 3, 4, 5, 6, 7 nm
Pd(6)/CMS(5)/Co(t_{Co})/Pd(3)	Co layer thickness: $t_{Co} = 0$, 1, 2, 3, 4, 5, 6 nm
Pd(6)/CMS(5)/Co(2)/Pd(t_{Pd})	Pd layer thickness: $t_{Pd} = 1$, 3, 5 nm
Pd(t_{Pd})/CMS(5)/Co(2)/Pd(1)	Pd layer thickness: $t_{Pd} = 4$, 5, 6, 7 nm

Table 2. Sputtering parameters for all targets.

Target	Power source (DC/RF)	Pressure (Pa)	Power (W)	Gas flow (sccm)	Substrate temperature (°C)
Pd	DC	0.5	15	Ar 20	350
CMS	DC	0.5	60	Ar 20	350
Co	DC	0.5	10	Ar 20	300, 350, 400, 450

3. Results and discussion

The Hall effect of magnetic materials includes the ordinary Hall effect (OHE) and anomalous Hall effect (AHE). The relationship between Hall resistance (R_{Hall}) and the perpendicular applied magnetic field H is as follows:

$$R_{Hall} = R_o H + 4\pi R_s M_\perp, \tag{1}$$

where $R_o H$ is the OHE and R_o is the ordinary Hall coefficient; $4\pi R_s M_\perp$ is the AHE portion, R_s is the anomalous Hall coefficient, and $M_\perp$ is the magnetization of the perpendicular film surface. Typically, the AHE in magnetic materials is more than an order of magnitude greater than the OHE, making the R_{Hall} approximately proportional to the magnetization of the perpendicular film surface.[30] Therefore, the magnetization characteristics of the perpendicular magnetic structure can be obtained from the relationship between R_{Hall} and the applied magnetic field H in the Hall curve. The abnormal Hall resistance is R_{Hall} at $H = 0$, which is marked R_{AHE}.

3.1. Research on PMA of Pd/Co/Pd trilayer layer films

Since CMS and Co are both magnetic materials, the basic structure of Pd/CMS/Pd and Pd/Co/Pd are first studied before studying the PMA of Pd/CMS/Co/Pd multilayer films. In our early research, the magnetic properties of Pd/CMS/Pd trilayer films have been studied,[29,31] so only the PMA of Pd/Co/Pd trilayer films is studied in this section.

3.1.1. Effect of Co layer thickness on PMA

Boeglin *et al*. reported that the PMA of Pd/Co/Pd trilayer films mainly comes from the destruction of interfacial symmetry and the orbital hybridization effect of the Pd 5d–Co 3d electrons,[32] and the interface effect is related to the thickness of the magnetic layer, so the Pd(6)/Co(t_{Co})/Pd(3) trilayer films are made at 400 °C. The influence of the Co layer thickness on the PMA characteristics of the trilayer films is investigated by measuring the Hall curve. Figure 1 shows the Hall curve of Pd(6)/Co(t_{Co})/Pd(3) trilayer films with different Co layer thicknesses. It can be found that the trilayer films show PMA property in the range of 1–2 nm Co layer thickness and no PMA property when $t_{Co} \leq 0.5$ nm and $t_{Co} \geq 3$ nm. When $t_{Co} \leq 0.5$ nm, because the Co layer is too thin to form a discontinuous film, the interface effect is poor, so the trilayer films do not show PMA. When $t_{Co} \geq 1$ nm, because a strong interface interaction can be formed at the Pd/Co interface, the interface magnetic anisotropy energy takes a larger proportion, and the interface magnetic property is greater than the bulk anisotropy energy, so the trilayer films show PMA.[29] When $t_{Co} = 1$ nm, the Hall curve has the best remanence ratio (the ratio of remanence M_r to saturated magnetization M_s) and large R_{Hall}. It indicates that the trilayer films have a strong PMA. With the increase of the Co layer thickness, the bulk anisotropy energy of the Co film gradually increases, and the proportion of the Pd/Co interface magnetic anisotropy energy gradually decreases. Therefore, the remanence ratio of the Hall curve of the trilayer films gradually decreases, and the PMA of the trilayer films gradually weakens. When $t_{Co} \geq 3$ nm, the bulk magnetic anisotropy energy of the Co film is greater than the Pd/Co interface magnetic anisotropy energy, so the PMA of the trilayer films disappears.

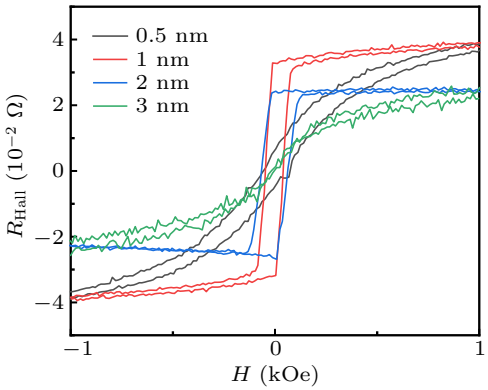


Fig. 1. Hall curves of Pd(6)/Co(t_{Co})/Pd(3) trilayer films with different Co layer thicknesses.

3.1.2. Effect of substrate temperature on PMA

Figure 2 shows the Hall curves of Pd(6)/Co(1)/Pd(3) trilayer films with different Co substrate temperatures. Only the substrate temperature of the Co layer is changed when preparing the Pd(6)/Co(1)/Pd(3) trilayer films. It can be observed that the trilayer films behave as PMA when the substrate temperature is between 350 °C and 400 °C. When the substrate temperature is lower than 300 °C and higher than 450 °C, the trilayer films do not show PMA properties. It is concluded that an appropriate substrate temperature can improve the crystal quality of the trilayer films, which makes the interface effect more obvious, and facilitates the production of the PMA of the trilayer films. When the substrate temperature is lower than 350 °C, the trilayer films do not show PMA because of the poor crystal quality and the weak interface quality. However, when the substrate temperature is too high, greater than 450 °C, the mutual diffusion of atoms at the adjacent interface is serious. At the same time, the grain grows synchronically, resulting in the increase of interface roughness and interface defects. The interface structure is destroyed, and the PMA of the trilayer films is weakened or even disappears.

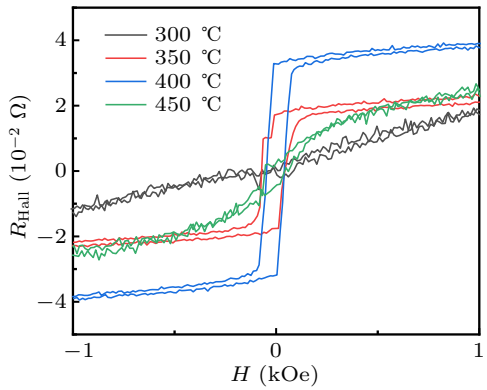


Fig. 2. Hall curves of Pd(6)/Co(1)/Pd(3) trilayer films with different Co substrate temperatures.

3.2. Effect of each film layer thickness on the PMA of Pd/CMS/Co/Pd multilayer films

3.2.1. Effect of Co layer thickness on PMA

The Hall curves of Pd(6)/CMS(5)/Co($t_{\rm Co}$)/Pd(3) multilayer films with different Co layer thicknesses are shown in Fig. 3(a). The relationship between the abnormal Hall resistance $R_{\rm Hall}$ ($H = 0$) and coercivity ($H_{\rm c}$) with the change of the Co layer thickness is shown in Fig. 3(b) shows. It can be seen from Fig. 3(a) that the multilayer films with Co layer thickness in the range of 0–5 nm exhibit PMA. When $t_{\rm Co} \geq 6$ nm, the multilayer films do not exhibit PMA properties. When $t_{\rm Co} \leq 2$ nm, the $R_{\rm Hall}$ of the multilayer films gradually increases with the gradual increase of the Co layer thickness; this is due to the gradual enhancement of CMS/Co interface FM coupling, magnetocrystalline anisotropy and magnetoelastic anisotropy.[26,33] Thus, the remanence ratio of the Hall curve of multilayer films is improved. When $t_{\rm Co} = 2$ nm, the remanence ratio of the Hall curve of multilayer films is close to 1 and has a large $R_{\rm Hall}$, which indicates that the multilayer films have a strong PMA. With the further increase of the Co layer thickness, the bulk anisotropy energy of the Co layer increases, resulting in a stepwise decreasing remanence ratio and a gradual weakening PMA of the multilayer films. Until $t_{\rm Co} \geq 6$ nm, the bulk anisotropy energy is greater than the interface magnetic anisotropy energy. Hence the PMA of the multilayer films disappears. However, the $H_{\rm c}$ of the multilayer films first increases and then decreases during the thickening of the Co layer. This is because the grain size grows synchronically with the increase of the thickness of the Co layer, which will increase the interface roughness, generating more defects. The number and size of the formed pinning points are also increased. Therefore the $H_{\rm c}$ of the multilayer films increases.[34] When the number of pinning points is higher than a certain degree, the coupling between particles will be reduced, which makes the $H_{\rm c}$ weaken.[35] In addition, the thickness of the Co layer in the optimal PMA multilayer films' structure is 1 nm higher than that in the Pd/Co/Pd trilayer films; this may be due to the diffusion of Co atoms at the CMS/Co interface. The diffusion of a certain amount of Co atoms to CMS increases the proportion of Co atoms in CMS, further enhancing the PMA of the multilayer films.[36]

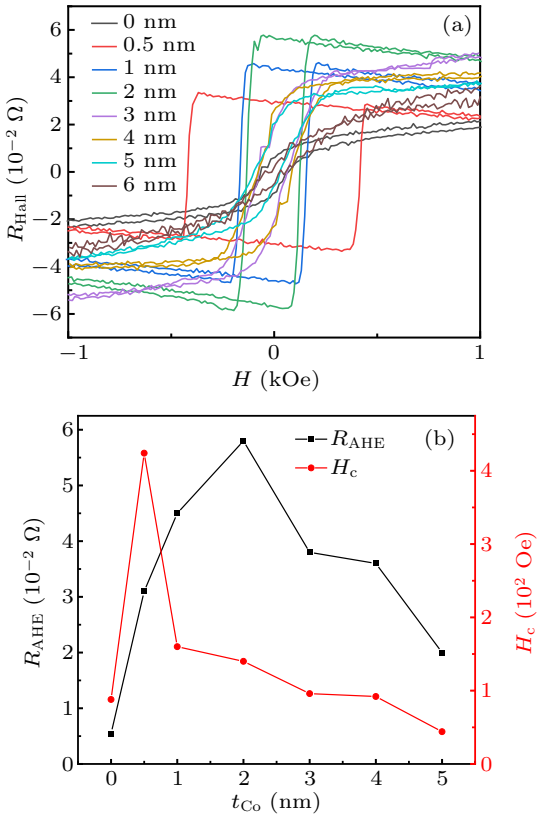


Fig. 3. (a) Hall curves of Pd(6)/CMS(5)/Co($t_{\rm Co}$)/Pd(3) multilayer films with different Co layer thicknesses. (b) The relationship between $R_{\rm Hall}$ (black) and $H_{\rm c}$ (red) of Pd(6)/CMS(5)/Co($t_{\rm Co}$)/Pd(3) multilayer films with the change of Co layer thickness.

3.2.2. Effect of CMS layer thickness on PMA

The Hall curves of Pd(6)/CMS(t_{CMS})/Co(2)/Pd(3) multilayer films with different CMS layer thicknesses are shown in Fig. 4(a). The relationship between R_{Hall} ($H = 0$) and H_c with the change of CMS layer thickness is shown in Fig. 4(b). Figure 4(a) shows that the multilayer films exhibit PMA properties in the range of 2–6 nm CMS layer thickness. When $t_{CMS} \leq 1$ nm and $t_{CMS} \geq 7$ nm, the multilayer films do not show PMA properties. When $t_{CMS} \leq 1$ nm, because the CMS layer is too thin, the film continuity is so poor that an effective interface effect is not produced, so the multilayer films do not show PMA property. When the thickness of the CMS layer is gradually increased, the film continuity and film quality are enhanced, and the CMS/Co interface FM coupling, magnetocrystalline anisotropy and magnetoelastic anisotropy are correspondingly enhanced.[26,33] The interface magnetic anisotropy energy gradually dominates. As a consequence, the PMA of the multilayer films appears and gradually strengthens. When $t_{CMS} = 5$ nm, the multilayer films have a good remanence ratio and a large R_{Hall}, indicating that the multilayer films have a strong PMA. With the CMS layer thickness increasing, the bulk anisotropy energy of the multilayer films is increasingly enhanced while the magnetocrystalline anisotropy and magnetoelastic anisotropy decrease, which makes the PMA of the multilayer films weaken. When $t_{CMS} \geq 7$ nm, the bulk anisotropy energy of the multilayer films dominates, and the PMA of the multilayer films disappears. The H_c of the multilayer films also increases first and then decreases during the thickening of the CMS layer, and the mechanism is the same as that during the thickening of the Co layer film.

Compared with the Pd(6)/Co(1)/Pd(3) trilayer films, the R_{Hall} of the Pd(6)/CMS(5)/Co(2)/Pd(3) multilayer films increased from 0.04 Ω to 0.058 Ω, an increase of 45%; the H_c increased from 48Oe to 140 Oe, an increase of 192%. The results detailed above show that the Pd(6)/CMS(5)/Co(2)/Pd(3) multilayer films have a stronger PMA than the Pd(6)/Co(1)/Pd(3) trilayer films. This is because the multilayer films have a variety of effects such as the orbital hybridization effect of Pd 5d–Co 3d electrons between the Pd/Co interfaces, FM coupling between the CMS/Co interfaces, and a strong interface magnetic anisotropy energy.

3.2.3. Effect of top Pd layer thickness on the PMA

The PMA of magnetic multilayer films is related not only to the interface magnetic anisotropy energy generated by interlayer coupling, but also to the thickness of the top Pd layer.[18,37] Figure 5(a) shows the Hall curve of the Pd(6)/CMS(5)/Co(2)/Pd(t_{Pd}) multilayer films with different top Pd layer thicknesses. Figure 5(b) shows the relationship between R_{Hall} ($H = 0$) and H_c with the change of the top Pd

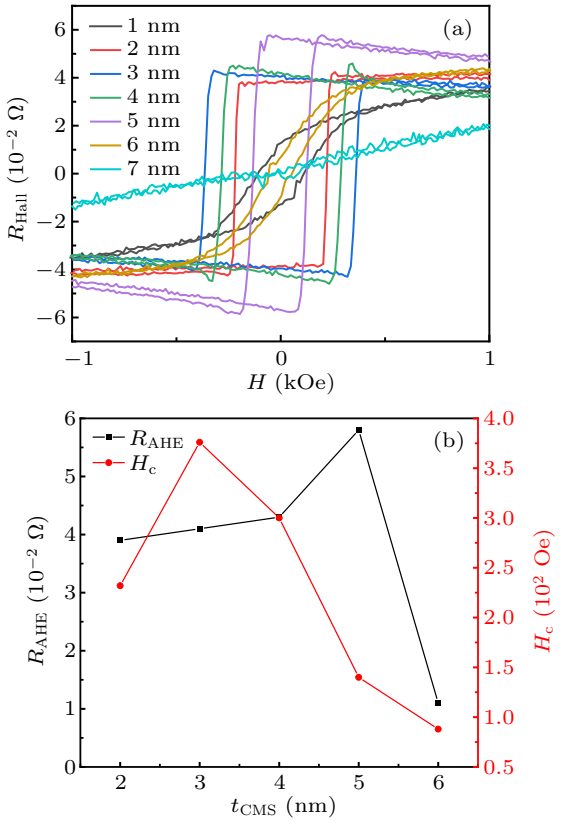


Fig. 4. (a) Hall curves of Pd(6)/CMS(t_{CMS})/Co(2)/Pd(3) multilayer films with different CMS layer thicknesses. (b) The relationship between R_{Hall} (black) and H_c (red) of Pd(6)/CMS(t_{CMS})/Co(2)/Pd(3) multilayer films with the change of the CMS layer thickness.

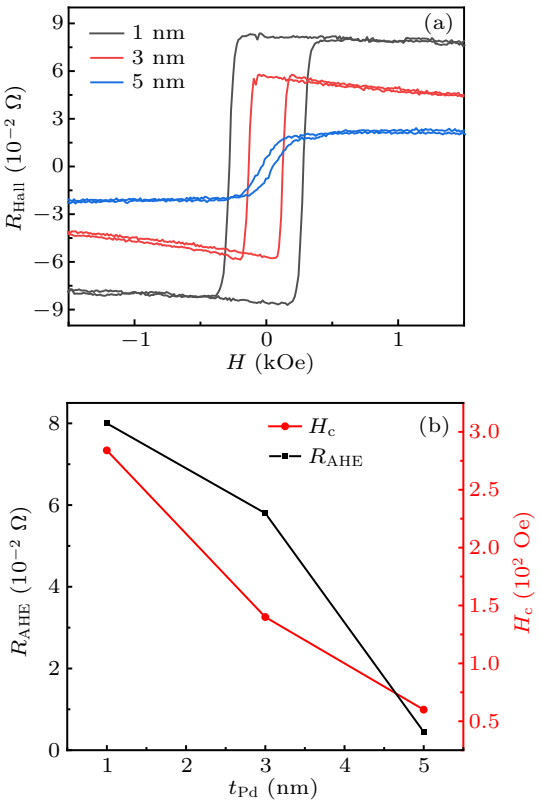


Fig. 5. (a) Hall curves of Pd(6)/CMS(5)/Co(2)/Pd(t_{Pd}) multilayer films with different top Pd layer thicknesses. (b) The relationship of R_{Hall} (black) and H_c (red) of Pd(6)/CMS(5)/Co(2)/Pd(t_{Pd}) multilayer films with the change of the top Pd layer thickness.

layer thickness. It can be seen from Fig. 5(a) that the remanence ratio of the multilayer films gradually decreases with the gradual increase of the top Pd layer thickness. This is attributed to Pd itself being a good conductor; the thickening of the top Pd layer will increase the shunt effect of the multilayer films, leading to the gradual decrease of the $R_{\rm Hall}$. While the $H_{\rm c}$ of the multilayer films decreases increasingly with the gradual increase of the thickness of the top Pd layer, the Pd atom is heavier than the Co atom. The bond cooperation of Pd is stronger than the Co atom. The Pd atom in the top protective layer is easier to diffuse into the Co layer.[18,37] Therefore, in a certain thickness range of the Pd layer, Co/Pd interface diffusion is proportional to the Pd layer thickness, which weakens the coupling effect between the Co layer and CMS layer, and reduces the PMA of the multilayer films. When the thickness of the top Pd layer is 1 nm, the multilayer films have a larger $R_{\rm Hall}$ and $H_{\rm c}$, and a better remanence ratio. The thickness of the top Pd layer is finally determined to be 1 nm.

3.2.4. Effect of bottom Pd layer thickness on PMA

The Hall curves of Pd($t_{\rm Pd}$)/CMS(5)/Co(2)/Pd(1) multilayer films with different bottom Pd layer thicknesses are shown in Fig. 6(a). The relationship between $R_{\rm Hall}(H=0)$ and $H_{\rm c}$ with the change of bottom Pd layer thickness is shown in Fig. 6(b). It can be seen from Fig. 6(a) that an appropriate substrate thickness is conducive to PMA generation in multilayer films. When $t_{\rm Pd} \leq 6$ nm, the remanence ratio, $R_{\rm Hall}$, $H_{\rm c}$, and PMA of the multilayer films all increase gradually with the gradual increase of the bottom Pd layer thickness. This is because the crystal quality and the texture of (111) (200) of the Pd layer are both enhanced[36] when the bottom Pd layer becomes thicker, which is conducive to the high quality growth of the subsequently sputtering CMS layer and Co layer. The interface quality of the multilayer films is also improved. The PMA of the multilayer films therefore gradually increases. When $t_{\rm Pd} = 6$ nm, the multilayer films have better remanence ratio and larger $R_{\rm Hall}$ and $H_{\rm c}$, indicating that the multilayer films have better PMA. When the thickness of the bottom Pd layer continues to increase, the grain size increase proceeds and the roughness and the defects are increased, which is adverse to the interface quality. Meanwhile, a Pd layer that is too thick will cause the interface magnetic anisotropy energy of the multilayer films to weaken, and the interface magnetic anisotropy energy to become less than the bulk anisotropy energy. The PMA of the multilayer films will therefore decrease. In addition, during the process of increasing the thickness of the bottom Pd layer in the multilayer films, the interfacial defects will increase, and the number of pinning points formed at the defects will increase. This will hinder the movement of domain walls, that is, the external field energy required for flipping the magnetic moment will increase, so the $H_{\rm c}$ of the multilayer films increases.[34] Finally, the thickness of the bottom Pd layer is determined to be 6 nm.

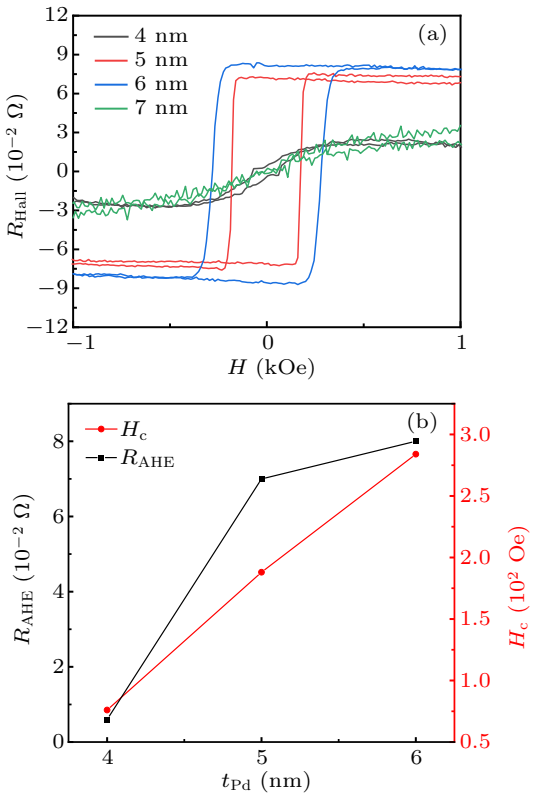


Fig. 6. (a) Hall curves of Pd($t_{\rm Pd}$)/CMS(5)/Co(2)/Pd(1) multilayer films with different bottom Pd layer thicknesses. (b) The relationship of $R_{\rm Hall}$ (black) and $H_{\rm c}$ (red) of Pd($t_{\rm Pd}$)/CMS(5)/Co(2)/Pd(1) multilayer films with the change of the bottom Pd layer thickness.

3.3. Effective PMA constant

To visually describe the strength of PMA in multilayer films, we introduce the effective PMA constant ($K_{\rm eff}$); the $K_{\rm eff}$ value can be estimated from the area difference between the in-plane and out-of-plane magnetization curves, namely,

$$K_{\rm eff} = \int_0^{H_{\rm s}} [M_\perp - M_\parallel]\,{\rm d}H,$$

where $M_\perp$ is the out-of-plane magnetization, $M_\parallel$ is the in-plane magnetization. In general, if the value of $K_{\rm eff}$ is positive, indicating that the multilayer films have PMA, the opposite is the in-plane magnetic anisotropy (IMA). The larger the $K_{\rm eff}$ value, the stronger the PMA of the multilayer films. Figure 7(a) shows the normalized in-plane and out-of-plane hysteresis loops of Pd(6)/CMS(5)/Co(2)/Pd(1) multilayer films. It can be observed from Fig. 7(a) that the remanence ratio of the out-of-plane hysteresis loops of the multilayer films is about 1, which is consistent with the results of the Hall curve. However the remanence ratio of the in-plane hysteresis loops is zero, and the saturation field is about 6.5 kOe. Figure 7(b) shows the unnormalized in-plane and out-of-plane hysteresis loops of Pd(6)/CMS(5)/Co(2)/Pd(1) multilayer films. It can be observed that the $M_{\rm s}$ value of the out-of-plane is about 784.2 emu/cm^3 and the $M_{\rm s}$ value of the in-plane is about 380.7 emu/cm^3. The $K_{\rm eff}$ value of Pd(6)CMS(5)/Co(2)/Pd(1) multilayer films is calculated to be 1.36 Merg/cm^3.

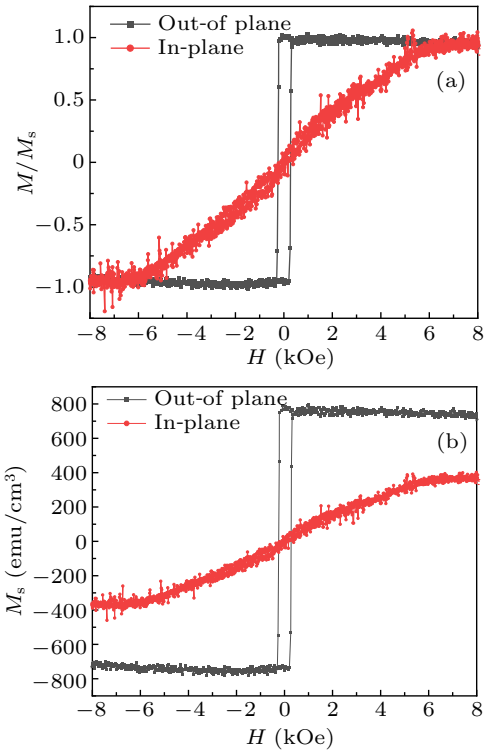


Fig. 7. (a) The normalized in-plane and out-of-plane hysteresis loops of Pd(6)/CMS(5)/Co(2)/Pd(1) multilayer films. (b) The unnormalized in-plane and out-of-plane hysteresis loops of Pd(6)/CMS(5)/Co(2)/Pd(1) multilayer films.

4. Conclusion

In this paper, a series of Pd/Co/Pd trilayer films and Pd/CMS/Co/Pd multilayer films are prepared by magnetron sputtering; the optimal PMA is obtained by optimizing the thickness of each layer and experimental parameters of the multilayer films. The main conclusions are as follows.

The Pd(6)/Co(t_{Co})/Pd(3) trilayer films can achieve PMA property in the range of 1–2 nm Co layer thickness. When $t_{Co} = 1$ nm and the substrate temperature is 400 °C, the Pd(6)/Co(1)/Pd(3) trilayer film has the strongest PMA. Its R_{Hall}, H_c and K_{eff} are 0.04 Ω, 48 Oe and 0.48 Merg/cm^3, respectively. The PMA of trilayer films is mainly due to the destruction of interfacial symmetry and the orbital hybridization effect of Pd 5d–Co 3d electrons.

The PMA of the Pd/CMS/Co/Pd multilayer films is studied by combining CMS film with high spin polarization and Co film with high PMA. The PMA of the multilayer films is greatly improved. The optimal structure of the multilayer films is Pd(6 nm)/CMS(5 nm)/Co(2 nm)/Pd(1 nm). Its R_{Hall}, H_c and K_{eff} are 0.08 Ω, 284 Oe and 1.36 Merg/cm^3, respectively, which are 100%, 492%, and 183% higher than those of the Pd (6 nm)/Co (1 nm)/Pd (3 nm) trilayer films.

The increase of the R_{Hall}, H_c and K_{eff} values is the result of the Pd/CMS interface effect and CMS/Co interface FM coupling, and it is closely related to the thickness of each film layer in the multilayer films and the growth conditions of the multilayer films.

Acknowledgement

Project supported by Shandong Provincial Natural Science Foundation, China (Grant No. ZR2022ME059).

References

[1] Draaisma H J G and de Jonge W J M de 1987 *J. Magn. Magn. Mater.* **66** 351
[2] Ikeda S, Miura K, Yamamoto H, Mizunuma K, Gan H D, Endo M, Kanai S, Hayakawa J, Matsukura and Ohno H 2010 *Nat. Mater.* **9** 721
[3] Sato H, Yamanouchi M, Ikeda S, Fukami S, Matsukura F and Ohno H 2012 *Appl. Phys. Lett.* **101** 022414
[4] Wang K, Tang Y, Liu J, You C Y and You L 2022 *Mater. Sci. Eng. B* **278** 115629
[5] Wen Z C, Sukegawa H, Mitani S and Inomata K 2011 *Appl. Phys. Lett.* **98** 242507
[6] Jodi M, Thomas L, Liu H L, Zhu J, Lee Y J, Le S, Tong R Y, Patel S and Sundar V 2019 *Sci. Rep.* **9** 19407
[7] Sahoo A K, Chelvane J and Mohanty J 2021 *Phys. Scr.* **96** 035803
[8] Thorarinsdottir K A, Thorbjarnardotti B R, Arnalds U B and Magnus F 2023 *J. Phys. Condens. Matter* **35** 205802
[9] Zhu L J and Ralph D C 2023 *Nat. Commun.* **14** 1778
[10] Liu Q B, Zhu L J, Zhang X, Muller D and Ralph D 2022 *Appl. Phys. Rev.* **9** 021402
[11] Peria W K, Katz M B, Wang J P, Crowell P and Gopman D B 2024 *Sci. Rep.* **14** 13290
[12] Wang X J, Krylyuk S, Josell D, Zhang D L, Lyu D, Wang J P and Gopman D B 2021 *AIP Adv.* **11** 025106
[13] Stellhorn A, Sarkar A, Kentzinger E, Waschk M, Schöffmann P, Schröder S, Abuladze G, Fu Z, Pipich V and Brückel T 2019 *J. Magn. Magn. Mater.* **476** 483
[14] Zhu L J, Nie S H, Xiong P, Schlottmann P and Zhao J H 2016 *Nat. Commun.* **7** 10817
[15] Hussain R, Aakansha, Brahma B, Basumatary R K, Brahma R, Ravi S and Srivastava S K 2019 *J. Supercond. Nov. Magn.* **32** 4027
[16] Li M H, Zhang S J, Wang S H, Li Y Z, Liu L, Chen Y, Shi H and Yu G H 2022 *Curr. Appl. Phys.* **34** 29
[17] Xiao X, Sun L, Luo Y M, Zhang D, Liang J H and Wu Y Z 2018 *J. Phys. D: Appl. Phys.* **51** 11500
[18] Won Y C and Lim S H 2021 *Sci. Rep.* **11** 10779
[19] Wen Z C, Sukegawa H, Mitani S and Inomata K 2011 *Appl. Phys. Lett.* **98** 242507
[20] Huang H B, Ma X Q, Liu Z H and Chen L Q 2014 *J. Alloys Compd.* **597** 230
[21] Bae T J, Ko J, Lee S, Cha J and Hong J 2016 *J. Appl. Phys.* **55** 013001
[22] Amari S, Mebsout R, Eçabih S M, Abbar B and Bouhafs B 2014 *Intermetallics.* **44** 26
[23] Wang K, Dong S, Xu Z and Huang Y 2016 *Mater. Lett.* **180** 140
[24] Liu Y W, Zhang J Y, Jiang S L, Liu Q Q, Li X J and Yu G H 2016 *J. Magn. Magn. Mater.* **420** 70
[25] Sbiaa R, Al-Omari I A, AlBahri M, Kharel P R, Ranjbar M, Akerman J and Sellmyer D J 2017 *J. Magn. Magn. Mater.* **441** 585
[26] Gottwald M, Girod S, Andrieu S and Mangin S 2010 *Mater. Sci. Eng.* **12** 012018
[27] Gladczuk L, Lasek K, Puzniak R, Sawicki M, Aleshkevych P, Paszkowica W, Minikayev R, Demchenko I N, Syryanyy Y and Przyslupski P 2017 *J. Phys. D* **50** 485002
[28] Tao X D, Liu Q, Mao B F, Yu R, Feng Z and Sun L, *et al.* 2018 *Sci. Adv.* **4** 1670
[29] Bai Q W, Jiang J, Guo B, Cao W T, Xiu X W and Wang S Y 2022 *J. Alloys Compd.* **897** 163114
[30] Nagaosa N, Sinova J, Onoda S, *et al.* 2010 *Rev. Mod. Phys.* **82** 1539
[31] Qin X Q, Guo B, Tan J X, Xiu X W, Cao W T and Wang S Y 2024 *J. Magn. Magn. Mater.* **600** 172143
[32] Boeglin C, Beaurepaire E, Haile V, Lopez-Flotrs V, Stamm C, Pontius N, Durr H A and Bigot J Y 2010 *Nature* **27** 465
[33] Arora M, Hubner R, Suess D, Heinrich B and Gir E 2017 *Phys. Rev. B.* **96** 024401
[34] Suzuki T, Notarys H, Dobbertin D C, *et al.* 1992 *IEEE Trans. Magn.* **28** 2754
[35] Sun A C, Hsu J H, Kuo P C, *et al.* 2007 *IEEE Trans. Magn.* **43** 2130
[36] Jiang J, Xiu X W, Wen K L, Cao W T, He Y and Wang S Y 2020 *J. Magn. Magn. Mater.* **505** 166709
[37] Lee T Y, Won Y C, Son D S, Lim S H and Lee S R 2014 *IEEE Magn. Lett.* **5** 1000104